JVI Journals.ASM.org

Analysis by Single-Gene Reassortment Demonstrates that the 1918 Influenza Virus Is Functionally Compatible with a Low-Pathogenicity Avian Influenza Virus in Mice

Li Qi, A. Sally Davis, Brett W. Jagger, Louis M. Schwartzman, Eleca J. Dunham, John C. Kash, and Jeffery K. Taubenberger

Viral Pathogenesis and Evolution Section, Laboratory of Infectious Diseases, National Institute of Allergy and Infectious Diseases, National Institutes of Health, Bethesda, Maryland, USA

The 1918-1919 "Spanish" influenza pandemic is estimated to have caused 50 million deaths worldwide. Understanding the origin, virulence, and pathogenic properties of past pandemic influenza viruses, including the 1918 virus, is crucial for current public health preparedness and future pandemic planning. The origin of the 1918 pandemic virus has not been resolved, but its coding sequences are very like those of avian influenza virus. The proteins encoded by the 1918 virus differ from typical low-pathogenicity avian influenza viruses at only a small number of amino acids in each open reading frame. In this study, a series of chimeric 1918 influenza viruses were created in which each of the eight 1918 pandemic virus gene segments was replaced individually with the corresponding gene segment of a prototypical low-pathogenicity avian influenza (LPAI) H1N1 virus in order to investigate functional compatibility of the 1918 virus genome with gene segments from an LPAI virus and to identify gene segments and mutations important for mammalian adaptation. This set of eight "7:1" chimeric viruses was compared to the parental 1918 and LPAI H1N1 viruses in intranasally infected mice. Seven of the 1918 LPAI 7:1 chimeric viruses replicated and caused disease equivalent to the fully reconstructed 1918 virus. Only the chimeric 1918 virus containing the avian influenza PB2 gene segment was attenuated in mice. This attenuation could be corrected by the single E627K amino acid change, further confirming the importance of this change in mammalian adaptation and mouse pathogenicity. While the mechanisms of influenza virus host switch, and particularly mammalian host adaptation are still only partly understood, these data suggest that the 1918 virus, whatever its origin, is very similar to avian influenza virus.

Influenza A viruses cause significant human morbidity and mortality, not only in the form of recurrent annual, or seasonal, influenza outbreaks but also as occasional and unpredictable pandemics (72). There have likely been at least 14 pandemics in the last 500 years (63) and four in the last 100 years, 1918 (H1N1), 1957 (H2N2), 1968 (H3N2), and 2009 (H1N1) (39). The worst pandemic in recorded history was the 1918-1919 "Spanish" influenza pandemic, estimated to have caused 50 million deaths worldwide and 675,000 deaths in the United States (26, 62). The emergence of a novel influenza A virus capable of causing a new pandemic is a major public health concern, especially with the continued circulation of Eurasian-lineage highly pathogenic avian influenza (HPAI) viruses of the H5N1 subtype capable of causing severe and unusually fatal respiratory disease in humans (44). The mechanisms of host switch, and particularly mammalian host adaptation, remain only partly understood, thus characterizing the origin, virulence, and pathogenic properties of past pandemic influenza viruses, including the 1918 virus, is crucial for current public health preparedness and future pandemic planning.

The natural reservoir of influenza A viruses (IAV) is thought to be numerous species of wild birds, predominantly of the orders *Anseriformes* and *Charadriiformes* (70). IAV adapted to humans and other mammalian species result from stable host switch events (43) in which novel influenza viruses either adapt *in toto* or by reassortment with human- or mammalian-adapted IAV (1, 11, 72). The mechanisms by which avian IAV stably adapt to mammalian hosts and the key mutations that allow efficient infectivity, replication, and transmission in the new species remain poorly understood despite significant research. Fitness barriers to viruses adapting to new hosts, including efficient viral replication and host-to-host transmissibility, may be selected for independently of changes associated with virulence and pathogenicity properties and might be associated with different and possibly conflicting or competing mutations (61).

Since human IAV had not yet been identified in 1918, no viral isolates were made during the 1918-1919 influenza pandemic. It was not until the modern molecular biology era that the genome of the 1918 pandemic virus could be sequenced from small viral RNA fragments retained in the lung tissues of victims of the 1918 pandemic virus (60) and reconstructed by reverse genetics to evaluate its pathogenicity in animal models (65). The 1918 virus is highly pathogenic in mice (28, 65), ferrets (37, 67), and cynomolgus macaques (29), causing significant morbidity and mortality in each of these species without prior adaptation. The 1918 virus also infects and replicates in the respiratory trees of swine (71) and guinea pigs (68) but without significant associated morbidity. In BALB/c mice, the best-studied experimental animal model of 1918 influenza virus pathogenicity, virulence has been shown to be polygenic in nature (28, 30, 42, 46, 65, 66, 69). These studies have demonstrated that both the gene encoding hemagglutinin (HA) and those encoding the ribonucleoprotein polymerase

Received 9 April 2012 Accepted 6 June 2012
Published ahead of print 20 June 2012
Address correspondence to Jeffery K. Taubenberger, taubenbergerj@niaid.nih.gov.

doi:10.1128/JVI.00887-12

(RNP) complex act as virulence factors in chimeric viruses in which one or more 1918 virus genes was inserted on the background of a contemporary human-adapted seasonal influenza virus.

Despite several studies, the origin of the 1918 pandemic virus has not been resolved (54, 56). Analysis of the GC content of the 1918 pandemic virus genome demonstrated that it is very similar to that of avian influenza virus (11, 47), as are the coding regions of the viral genes. This has facilitated prediction of mutations that might be associated with human adaptation (13, 38, 64). The proteins encoded by the 1918 virus differ from the proteins encoded by typical low-pathogenicity avian influenza (LPAI) viruses at only a small number of amino acids encoded by each open reading frame. In this study, we created a series of chimeric 1918 influenza viruses in which each of the eight 1918 gene segments was replaced individually with the corresponding gene segment of a prototypical LPAI virus in order to assess functional compatibility of the 1918 viral genome with genes from an LPAI virus and to identify gene segments and mutations important for mammalian adaptation. This set of eight "7:1" chimeric viruses (each containing seven 1918 pandemic virus gene segments and one low-pathogenicity avian influenza gene segment) was compared to the parental 1918 and LPAI H1N1 viruses *in vivo* in intranasally infected mice.

MATERIALS AND METHODS

Virus preparation. The fully reconstructed 1918 H1N1 influenza virus (hereafter referred to as 1918) was prepared using a standard reverse genetics system as previously described (12, 46). A low-pathogenicity avian H1N1 influenza virus plasmid rescue set (hereafter referred to as AI) was similarly constructed using the cloned gene segments (excluding the hemagglutinin [HA] gene segment) from A/Green Wing Teal/Ohio/175/1986 (H2N1) and the HA segment from A/mallard/Ohio/265/1987 (H1N9); viruses were kindly supplied by Richard Slemons, Ohio State University (10). These viruses were chosen because the genes of the H2N1 virus were each very similar to the avian influenza virus consensus (see below), as was the HA gene of the H1N9 virus. The rescued "consensus" H1N1 AI virus grew to comparable titers in both eggs ($\sim 1 \times 10^6$ PFU/ml) and Madin-Darby canine kidney (MDCK) cells ($\sim 2 \times 10^6$ PFU/ml) to both the parental A/Green Wing Teal/Ohio/175/1986 (H2N1) and A/mallard/Ohio/265/1987 (H1N9) viruses. The percent identity of the proteins encoded by the major open reading frames of the 1918 and AI H1N1 viruses compared to the avian consensus sequences and between the 1918 and AI viruses is shown in Table 1.

A set of eight chimeric rescued "7:1" influenza viruses were generated in which each of the eight gene segments from 1918 was replaced individually with the corresponding gene segment from AI (1918:AI viruses). These 7:1 viruses were denoted as $1918^{\text{AI-PB2}}$, $1918^{\text{AI-PB1}}$, $1918^{\text{AI-PA}}$, $1918^{\text{AI-HA}}$, $1918^{\text{AI-NP}}$, $1918^{\text{AI-NA}}$, $1918^{\text{AI-M}}$, and $1918^{\text{AI-NS}}$. A 1918 virus with the PB2 K627E mutation [($1918^{\text{PB2-E627}}$)] and a corresponding chimeric 1918 virus with AI PB2 E627K mutation ($1918^{\text{AI-PB2-K627}}$) were also generated. These viruses are listed in Table 2.

All rescued viruses were propagated once in Madin-Darby canine kidney cells (ATCC, Manassas, VA). The genomic sequence of each rescued virus was then confirmed by sequence analysis of the inoculum. All viruses and infectious samples were handled under enhanced biosafety level 3 (BSL-3) laboratory conditions, and experiments with the fully reconstructed 1918 pandemic virus were conducted in accordance with the select agent guidelines of the National Institutes of Health and the Centers for Disease Control and Prevention and under the supervision of the NIH Select Agent and Biosurety Programs and the NIH Department of Health and Safety.

Mouse infections. All experimental animal work was performed in an enhanced animal BSL-3 (ABSL-3) laboratory at the National Institute of Allergy and Infectious Diseases (NIAID) following animal safety protocols approved by the NIAID Animal Care and Use Committee and the Select Agent guidelines of the National Institutes of Health and the Centers for Disease Control and Prevention. Groups of five 8- to 10-week-old female BALB/c mice (Jackson Laboratory, Bar Harbor, ME) were lightly anesthetized in a chamber with isoflurane supplemented with O_2 (1.5 liters/min) prior to intranasal inoculation with virus in a total volume of 50 μl. Viruses were diluted in sterile Dulbecco modified Eagle medium (DMEM) where appropriate. Survival and body weight were monitored for up to 14 days, and mice were humanely euthanized if more than 25% starting body weight was lost. Mouse 50% lethal doses (MLD_{50}) were determined by inoculating groups of five mice with serial 10-fold dilutions of virus. MLD_{50} were calculated by the method of Reed and Muench (49) and are expressed as the $\log_{10}$ PFU required to give 1 MLD_{50}. For the comparative pathogenesis study, groups of 5 mice were inoculated intranasally with 1,000 PFU of each virus. On days 1, 3, and 5 postinoculation, lungs from 3 animals were collected for viral titration and 2 animals for pathology from each virus group. Lung viral titers were determined by plaque assay (described above) in 10% (wt/vol) lung suspensions prepared by homogenization in sterile 1× L15 medium. Lungs collected for pathology were inflated with 10% neutral buffered formalin (NBF) at time of harvest in order to prevent atelectasis.

Pathology, immunohistochemistry, and digital microscopy. Following fixation for at least 24 h in 10% NBF, lung tissue samples were dehydrated and embedded in paraffin. All stains were done on 5-μm sections placed on positively charged slides (American Histolabs, Gaithersburg, MD, and Histoserv Inc., Germantown, MD). Hematoxylin and eosin (H&E)-stained slides were examined for each mouse. Immunohistochemistry (IHC) for influenza A antigen using goat polyclonal anti-H1N1 (ab20841; Abcam, Cambridge, MA) and neutrophils using rabbit polyclonal antimyeloperoxidase (PU496-UP; BioGenex, Freemont, CA) were completed on a subset of tissues (North Carolina State University [NCSU] College of Veterinary Medicine [CVM] Histology Laboratory, Raleigh, NC). For influenza virus antigen labeling, the slides were deparaffinized and rehydrated, antigen was retrieved in pH 6 citrate buffer in a pressure cooker, blocked with 3% hydrogen peroxide on a Dako Autostainer Plus (S3800; Dako), serum blocked, incubated first for 30 min with 1:300 dilution of primary antibody, for 10 min with secondary antibody (PK-6105; Vector Labs, Burlingame, CA), and for 10 min with streptavidin-conjugated peroxidase (K0675; Dako) with intermediary Tris buffer rinses. For myeloperoxidase IHC, the slides were deparaffinized, rehydrated, incubated overnight at 4°C with 1:10 primary antibody, and then detected with biotinylated anti-rabbit immunoglobulins followed by streptavidin peroxidase (HK326-UR and HK320-UK; BioGenex) each at a 1:20 dilution for 20 min each. Both markers were visualized with 3,3′-diaminobenzidine (DAB+) chromogen substrate (catalog no. K3468; Dako), and then the slides were rinsed, dehydrated, and mounted.

All slides were scanned on an Aperio ScanScope XT system (Aperio, Vista, CA) enabling whole-slide analysis. Two pathologists reviewed these slides, one independently using a light microscope in a blinded fashion and then both together digitally reaching consensus on the presented findings. The related figures presented in this paper were extracted from these digital slides and compiled into multipanel images using Adobe Photoshop CS4 (Adobe, San Jose, CA). Additionally, a subset of myeloperoxidase (MPO) slides for the day 5 time point was analyzed digitally using Aperio algorithms. First, the Color Deconvolution algorithm version 9 was applied to adjust for the specific DAB and hematoxylin stain color characteristics and intensity consistent with pathologist-validated cytoplasmic labeling of neutrophils. Then after the whole slide was marked up to eliminate the nonpulmonary tissue and the airways down to the level of the terminal bronchioles, the colocalization algorithm version 9 was adjusted based on the Color Deconvolution algorithm outputs applied to the slides of interest, producing a percentage of analyzed pulmonary tissue positive for the MPO label as a result for each slide.

TABLE 1 Comparison of 1918 and AI major coding sequences with the avian influenza A virus consensus sequence

Protein	Amino acid difference(s) from the avian influenza A virus consensus sequence (amino acid identity; %)[a]		Amino acid differences between AI and 1918 viruses (amino acid identity; %)[b]
	AI virus	1918 virus[b]	
Influenza virus proteins			
PB2	2 (757/759; 99.7); K187R, M402L	9 (750/759; 98.8); T108A, V114I, **A199S**, **L475M**, I478V, I539V, **D567N**, **E627K**, **K702R**	11 (748/759; 98.6); T108A, V114I, K187R, **A199S**, M402L, **L475M**, I478V, I539V, **D567N**, **E627K**, **K702R**
PB1	0 (757/757; 100)	7 (750/757; 99.1); K54R, **N375S**, E383D, V473L, L576I, V645M, S654N	7 (750/757; 99.1); K54R, **N375S**, E383D, V473L, L576I, V645M, S654N
PA	6 (710/716; 99.2); I62L, V323I, S388G, I423M, A476V, E630V	10 (706/716; 98.6); **P28L**, **D55N**, **V100A**, C241Y, K312R, I322V, **E382D**, P400L, **T552S**, K716R	16 (700/716; 97.8); **P28L**, **D55N**, I62L, **V100A**, C241Y, K312R, I322V, V323I, **E382D**, S388G, P400L, I423M, A476V, **T552S**, E630V, K716R
NP	1 (497/498; 99.8); N417S	9 (489/498; 98.2); **G16D**, **V33I**, **R100I**, **L136M**, **L283P**, **F313Y**, **Q357K**, N450S, N473S	10 (488/498; 98.0); **G16D**, **V33I**, **R100I**, **L136M**, **L283P**, **F313Y**, **Q357K**, N417S, N450S, N473S
M1	0 (252/252; 100)	2 (250/252; 99.2); **T121A**, L235I	2 (250/252; 99.2); **T121A**, L235I
M2	0 (97/97; 100)	5 (92/97; 94.9); **G14E**, **E16G**, **K18R**, **S20N**, Q78K	5 (92/97; 94.9); **G14E**, **E16G**, **K18R**, **S20N**, Q78K
NS1	1 (229/230; 99.6); M119I	4 (229/230; 99.6); E70K, I178V, D209N, **E227K**	5 (225/230; 97.8); E70K, I119M, I178V, D209N, **E227K**
NEP (NS2)	0 (121/121; 100)	1 (120/121; 99.2); S60N	1 (120/121; 99.2); S60N
Surface glycoproteins			
HA (H1 subtype)	7 (559/566; 98.8); S53N, N138S, T173N, T202A, T212A, R295K, K467R	43 (523/566; 92.4); K4R, F6L, F9L, T11A, T13A, V14A, L15T, K16N, V22I, S60K, N62K, V74I, **N91S**, I97V, E111D, A137T, N138S, **S156A**, I168L, **T173S**, **T183V**, **T202G**, **S203T**, **E204D**, **G239D**, **D252E**, **Q253P**, K276R, D279G, N291D, D293N, R295K, L303I, V312I, I315V, K325R, V338I, V435I, R467K, R471K, L477I, E491A, K497R	41 (525/566; 92.8); K4R, F6L, F9L, T11A, T13A, V14A, L15T, K16N, V22I, N53S, S60K, N62K, V74I, **N91S**, I97V, E111D, A137T, **S156A**, I168L, **N173S**, **T183V**, **A202G**, **S203T**, **E204D**, **G239D**, **D252E**, **Q253P**, K276R, D279G, N291D, D293N, L303I, V312I, I315V, K325R, V338I, V435I, R471K, L477I, E491A, K497R
NA (N1 subtype)	10 (459/459; 97.9) V16A, V80I, V83M, P93S, N222D, N270S, S286G, Q313R, V357A, S385N	32 (437/469; 93.2) I17V, V23I, S42N, V53I, I67V, **L74V**, I75V, **E77G**, **A79D**, V80A, **A81T**, P82S, **T84I**, A86T, **I188M**, S189G, I234V, F256L, V264T, **V267I**, **A285T**, S286G, **E287K**, **N307D**, E311D, **Y344N**, V346I, **K352R**, G354D, K390R, R430Q, T466S	39 (430/469; 91.7) A16V, I17V, V23I, S42N, V53I, I67V, **L74V**, I75V, **E77G**, **A79D**, I80A, **A81T**, P82S, M83V, **T84I**, A86T, S93P, **I188M**, S189G, D222N, I234V, F256L, V264T, **V267I**, S270N, **A285T**, **E287K**, **N307D**, E311D, R313Q, **Y344N**, V346I, **K352R**, G354D, A357V, N385S, K390R, R430Q, T466S

[a] Avian influenza consensus sequences were determined as described in Materials and Methods. The number of amino acid differences and then the amino acid differences are listed. After the number of amino acid differences, amino acid identity is indicated by the number of identical amino acids to the total number of amino acids and the percentage in parentheses.

[b] Amino acid changes previously identified as possible mammalian adaptation mutations are shown in boldface type (7, 13, 50–53, 64).

Statistical analysis. Mortality and the average number of days postinoculation (dpi) until death or endpoint euthanasia were analyzed by using analysis of variance (ANOVA) in GraphPad Prism version 5.0 (GraphPad Software Inc., La Jolla, CA); a P value of 0.05 or less was considered significant. Response variables that varied significantly by treatment group were further subjected to comparisons for all pairs by using the Tukey-Kramer test. Pairwise mean comparisons between inoculated and control groups were made using the Student t test.

Sequence analysis. The 1918 and AI gene sequences were compared to consensus wild-bird-derived influenza virus sequences downloaded from the Influenza Virus Resource database (4).

North American and Eurasian avian sequences were downloaded from the Influenza Virus Resource database (http://www.ncbi.nlm.nih.gov/genomes/FLU/FLU.html). The data set excluded gallinaceous avian sequences. Consensus sequences were obtained after manually aligning the coding regions of each gene segment using Se-Al (48). Sequence alignments consisted of the following coding regions for each segment: 1,116 PB2 (2,277-nucleotide [nt]) sequences, 1,116 PB1 (2,271-nt) sequences, 1,119 PA (2,148-nt) sequences, 212 HA (1,218-nt) sequences, 1,119 NP (1,494-nt) sequences, 865 neuraminidase (NA) (1,410-nt) sequences, 514 M1/2 (1,002-nt) sequences, and 550 NS1/2 (831-nt) sequences. These sequence alignments are available upon request. Sequence comparisons were performed by aligning the 1918, AI H1N1, and avian influenza virus consensus protein sequences in MegAlign (DNAStar Inc., Madison, WI), and these sequence alignments are available upon request.

RESULTS

Sequence comparisons between the 1918 and AI viruses. The protein sequences encoded by the low-pathogenicity H1N1 avian

TABLE 2 Properties of parental and 7:1 chimeric viruses used in this study

Virus	Origin of segment[a]								MLD_{50}[b]	Lung titer (mean ± SEM) at the following time[b,c]:			MDCK titer[b]
	PB2	PB1	PA	HA	NP	NA	M	NS		1 dpi	3 dpi	5 dpi	
1918									2.1	5.6 ± 0.2	6.8 ± 0.0	6.6 ± 2.2	8.0
$1918^{AI\text{-}PB2}$									>5.0	2.3 ± 1.1	4.3 ± 0.0	4.3 ± 1.1	6.9
$1918^{AI\text{-}PB1}$									1.8	6.5 ± 0.3	6.5 ± 0.1	5.9 ± 0.3	7.7
$1918^{AI\text{-}PA}$									1.8	5.1 ± 0.3	5.7 ± 0.1	6.0 ± 0.2	7.6
$1918^{AI\text{-}HA}$									1.4	4.9 ± 0.3	5.6 ± 0.3	5.2 ± 0.2	7.0
$1918^{AI\text{-}NP}$									2.1	5.9 ± 0.1	6.1 ± 0.2	5.3 ± 0.1	7.9
$1918^{AI\text{-}NA}$									2.7	5.4 ± 0.4	5.9 ± 0.1	5.2 ± 0.1	7.6
$1918^{AI\text{-}M}$									2.7	6.4 ± 0.1	6.3 ± 0.1	5.7 ± 0.4	7.2
$1918^{AI\text{-}NS}$									2.3	5.7 ± 0.1	6.3 ± 0.3	6.3 ± 0.1	7.7
AI									>5.0	BD	BD	BD	7.4
$1918^{PB2\text{-}E627}$	E627								>5.0	ND	ND	5.6 ± 0.3	6.1
$1918^{AI\text{-}PB2\text{-}K627}$	K627								1.8	5.9 ± 0.2	6.4 ± 0.4	5.7 ± 0.3	7.7

[a] Thrste origin of each of the eight gene segments is shown by shading (originated from the 1918 virus) or lack of shading (originated from the AI virus). For the first virus, the 1918 pandemic influenza virus, all eight of the gene segments were from the 1918 virus and are shaded. For the second virus listed, the $1918^{AI\text{-}PB2}$ virus, the PB2 gene segment was from the AI virus (not shaded) and the remaining seven gene segments were from the 1918 virus (shaded).
[b] Data presented as $\log_{10}$ PFU.
[c] BD, below the limit of detection. ND, not done.

influenza (AI) virus used in this study were compared to the protein sequences encoded by the avian influenza virus consensus sequence (see Materials and Methods) and to those encoded by the 1918 influenza virus (Table 1). The AI virus genome had a very high sequence identity to the avian consensus sequences, differing in total in 17/1,025 amino acids (98.3% identity) in the hemagglutinin (HA) and neuraminidase (NA) surface glycoproteins and in only 10/3,430 (99.7% identity) amino acids out of the eight remaining major open reading frames ("internal" proteins). Overall, the AI virus matched the avian influenza virus consensus sequence at 4,428/4,455 amino acids (99.4% identity), confirming that this virus was highly representative of low-pathogenicity avian influenza viruses.

The 1918 virus differed from the AI virus in 57/3,430 amino acids of the internal proteins (98.3% identity) and in 80/1,025 amino acids of the HA and NA (92.2% identity). Overall, the 1918 virus was identical to the AI virus in 4,318/4,455 amino acids (96.9% identity). Of the 57 amino acid differences in the internal proteins, 23 (40.4%) have been previously reported as possible mammalian-adaptive changes (Table 1). Similarly, 22 of the 80 amino acid differences in the HA and NA (27.5%) had been associated with mammalian adaptation (Table 1). We next sought to determine which of the preceding changes were important in mammalian adaptation of the 1918 virus in an *in vivo* mouse model.

Comparison of 1918 and 1918:AI 7:1 chimeric viruses in a mouse infection model. To determine which avian gene segments would confer attenuation to the 1918 virus in a mouse model, we studied the growth and pathogenicity of 8 chimeric reassortant influenza viruses in which each of the eight segments of the parental 1918 pandemic H1N1 was individually replaced with the corresponding segment derived from AI (1918:AI 7:1). All the viruses grew to comparable titers in MDCK cells (Table 2). As previously shown (12), the fully reconstructed control 1918 virus at 10^3 PFU caused a lethal infection in mice (8 times the calculated MLD_{50} dose for the 1918 virus; Table 2), whereas the AI parental H1N1 virus caused no significant weight loss and all infected mice survived. Intriguingly, except for the $1918^{AI\text{-}PB2}$ chimeric virus, all other 1918:AI 7:1 viruses showed weight loss kinetics similar to the fully reconstructed 1918 virus (Fig. 1). Similarly, these viruses were all lethal in mice at this dose, with 100% of infected mice either dying or reaching endpoint criteria between 6 and 10 dpi. In contrast, mice inoculated with the $1918^{AI\text{-}PB2}$ virus showed only mild, transient weight loss (5% maximum), and none died (Fig. 1). Viral lung titers at 1, 3, and 5 dpi are shown in Table 2. All the 1918:AI chimeric 7:1 viruses replicated in mouse lung, but only the $1918^{AI\text{-}PB2}$ virus showed a statistically significant decrease in titer at 1 dpi ($P = 0.028$), 3 dpi ($P < 0.001$), and 5 dpi ($P = 0.005$) compared to 1918 (Table 2), with titers 2 to 3 $\log_{10}$ PFU lower at each time point tested. The AI virus did not replicate to detectable titers in mouse lung.

Given these results, a comparative MLD_{50} study of these vi-

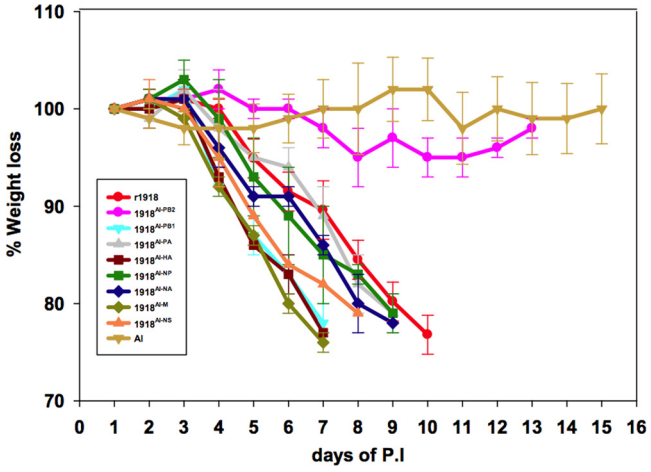

FIG 1 Weight loss of mice infected with parental 1918 influenza and AI viruses and eight chimeric 7:1 1918 influenza viruses bearing each of the gene segments of the AI H1N1 virus, respectively. Seven- to eight-week-old female BALB/c mice were intranasally inoculated with 10^3 PFU of the indicated viruses (see Table 2 and color-coded key) and weighed daily (5 mice per virus per group). P.I., postinoculation.

ruses was performed (Table 2). The MLD_{50} of the AI parental control virus could not be determined, as it was nonlethal at 10^5 PFU, the highest dose tested. Each of the 7 chimeric 1918:AI viruses that caused lethal infections in the initial experiment had an MLD_{50} similar to that of the fully reconstructed 1918 virus. In contrast, the $1918^{AI\text{-}PB2}$ virus was nonlethal to mice even at a dose of 10^5 PFU (Table 2). Taken together, these results demonstrated that only the chimeric 7:1 $1918^{AI\text{-}PB2}$ virus with the AI PB2 gene segment was able to significantly attenuate the replication and pathogenicity of the 1918 virus in mice.

Lung histopathology of mice infected with AI, 1918, and 7:1 chimeric viruses at 5 dpi. Infection with the parental AI virus resulted in no pathological changes in the respiratory tract (Fig. 2A). Rare bronchial epithelial cells were positive for influenza virus antigen in the lungs of AI virus-infected mice (Fig. 2B). As previously described (12), infection with the fully reconstructed 1918 virus resulted in a severe transmural necrotizing bronchiolitis and multifocal moderate-to-severe alveolitis with multifocal pulmonary edema (Fig. 2C). The alveolar inflammatory infiltrates were of mixed cellularity, and neutrophils were commonly observed. Correlating to the marked histopathological changes in these infections, abundant influenza virus antigen was observed in both bronchiolar and alveolar epithelial cells as described previously (12) (Fig. 2D).

Of the mice infected with chimeric 7:1 viruses, seven of them had weight loss, MLD_{50}, and lung titers during the course of infection that were comparable to those of the parental 1918 virus: $1918^{AI\text{-}PB1}$, $1918^{AI\text{-}PA}$, $1918^{AI\text{-}HA}$, $1918^{AI\text{-}NP}$, $1918^{AI\text{-}NA}$, $1918^{AI\text{-}M}$, and $1918^{AI\text{-}NS}$ (Table 2). Histopathological examination in mice infected with each of these viruses showed similar patterns of severe necrotizing bronchiolitis and multifocal moderate-to-severe alveolitis with multifocal pulmonary edema not significantly different from those of the parental 1918 virus. Viral antigen distribution in each case was widespread in bronchiolar and alveolar epithelial cells comparable to that observed in the parental 1918 virus (12; also data not shown). In contrast, the $1918^{AI\text{-}PB2}$ virus, as expected given its attenuated phenotype in mice, induced in aggregate no histologic changes (Fig. 2E) except rare small foci of mild bronchiolitis. Interestingly, given its lack of inflammatory changes, viral antigen was noted throughout both bronchiolar and alveolar epithelia, although to a lesser degree than in parental 1918 virus-infected mice (Fig. 2F).

Comparison of viruses with mutations at PB2 amino acid 627 in mice. With the unexpected finding that only one of the eight 1918:AI 7:1 viruses had a markedly attenuated phenotype in mice (the $1918^{AI\text{-}PB2}$ virus), experiments were designed to explore the molecular basis of this observation. A computational translation of the 1918 PB2 open reading frame showed that it differed at 11 codons from a translation of PB2 of the AI virus used in this study (Table 1). Of these 11 coding mutations, 5 had been previously hypothesized to be potential mammalian-adaptive mutations (64), including the E627K mutation long associated with mammalian adaptation (58) and virulence of some highly pathogenic H5N1 viruses in mice (21). Avian influenza viruses generally encode a glutamic acid (E) at this site, while 1918 virus lineage human isolates typically encode a lysine (K). A set of viruses was therefore constructed with mutations at PB2 codon 627 to test whether changes at this single amino acid change would alter the observed viral replication ability or pathogenicity in mice (Table 2). Compared to the 1918 parental virus, a mutant isogenic 1918 virus ($1918^{PB2\text{-}E627}$) with the single 1918 PB2 change of K627E (back to the avian influenza consensus codon), was markedly attenuated in mice, causing neither appreciable weight loss (Fig. 3) nor mortality. In contrast, a 7:1 chimeric $1918^{AI\text{-}PB2}$ virus construct with the single PB2 E627K change ($1918^{AI\text{-}PB2\text{-}K627}$) was pathogenic in mice (Fig. 3) and replicated to titers and had an MLD_{50} comparable to those of the parental 1918 virus (Table 2). These data show that the single PB2 E627K mutation in either the 1918-derived PB2 or an AI-derived PB2 gene was adequate to confer replication and murine pathogenicity similar to the 1918 virus in these chimeric viruses in the absence of other PB2 mutations. While both the $1918^{AI\text{-}PB2}$ and $1918^{PB2\text{-}E627}$ viruses were markedly attenuated compared to the other 1918^{AI} chimeric viruses (Table 2), these viruses replicated in mouse lung, in contrast with the parental AI virus. To assess whether the PB2 codon 627 might have been under selection pressure to mutate during the $1918^{AI\text{-}PB2}$ infection in mice, the PB2 gene was amplified and sequenced by reverse transcription-PCR (RT-PCR) from RNA isolated from 25 individual plaques derived from culture of a mouse lung at dpi 5. As has been reported in other systems (5), K627 revertants were observed in 23 of 25 plaques (92%) from the $1918^{AI\text{-}PB2}$ (E627) virus-infected mouse lung. In 3 of the 23 plaques with PB2 K627, another coding change, D611N, was also observed.

Comparison of 1918 and $1918^{AI\text{-}HA}$ viruses in a mouse infection model. The 1918 HA has been previously identified as a virulence factor in chimeric viruses constructed on the background of various human seasonal influenza viruses in mice and ferrets (30, 42, 45, 46). As described above, the 7:1 chimeric 1918 virus with the HA gene derived from the AI virus ($1918^{AI\text{-}HA}$) was not attenuated in either its replication or pathogenicity in mice in these experiments. Histopathologically, there were no appreciable differences between the 1918 and $1918^{AI\text{-}HA}$ viruses (Fig. 2). Because acute alveolitis with a prominent neutrophil infiltrate is a known feature associated with the pathogenesis of the 1918 virus or viral constructs containing the 1918 HA in animal models (45, 46, 65), we sought to evaluate whether there were differences in the alveolar infiltrates between these viruses. Myeloperoxidase-labeled neutrophils in alveolar tissues were assessed using digital microscopy (see Materials and Methods). However, no differences in neutrophil infiltrates were noted between 1918 parental and $1918^{AI\text{-}HA}$ viruses by histopathologic review or digital analysis of the MPO labeling (Fig. 4). Therefore, at least in the context of the other seven 1918 genes, a low-pathogenicity avian HA could elicit responses similar to the 1918 HA protein.

DISCUSSION

The origin of the 1918 pandemic influenza H1N1 virus has not been resolved by phylogenetic analyses (3, 20, 54, 57, 64), and it may not be understood until precursor viruses are identified through archaevirologic studies. Whatever its origin, the 1918 viral genome is very similar to avian influenza virus in its genome composition (11, 47) and coding sequences (13, 38, 64). In this study, we sought to assess the functional compatibility of the 1918 viral genome with gene segments derived from an LPAI virus and also to identify genes associated with mammalian adaptation in a mouse model. The "internal" proteins encoded by the 1918 virus differed by between 1 and 11 mutations each compared to the proteins encoded by a typical LPAI virus. A large number of these changes have been previously reported to be associated with

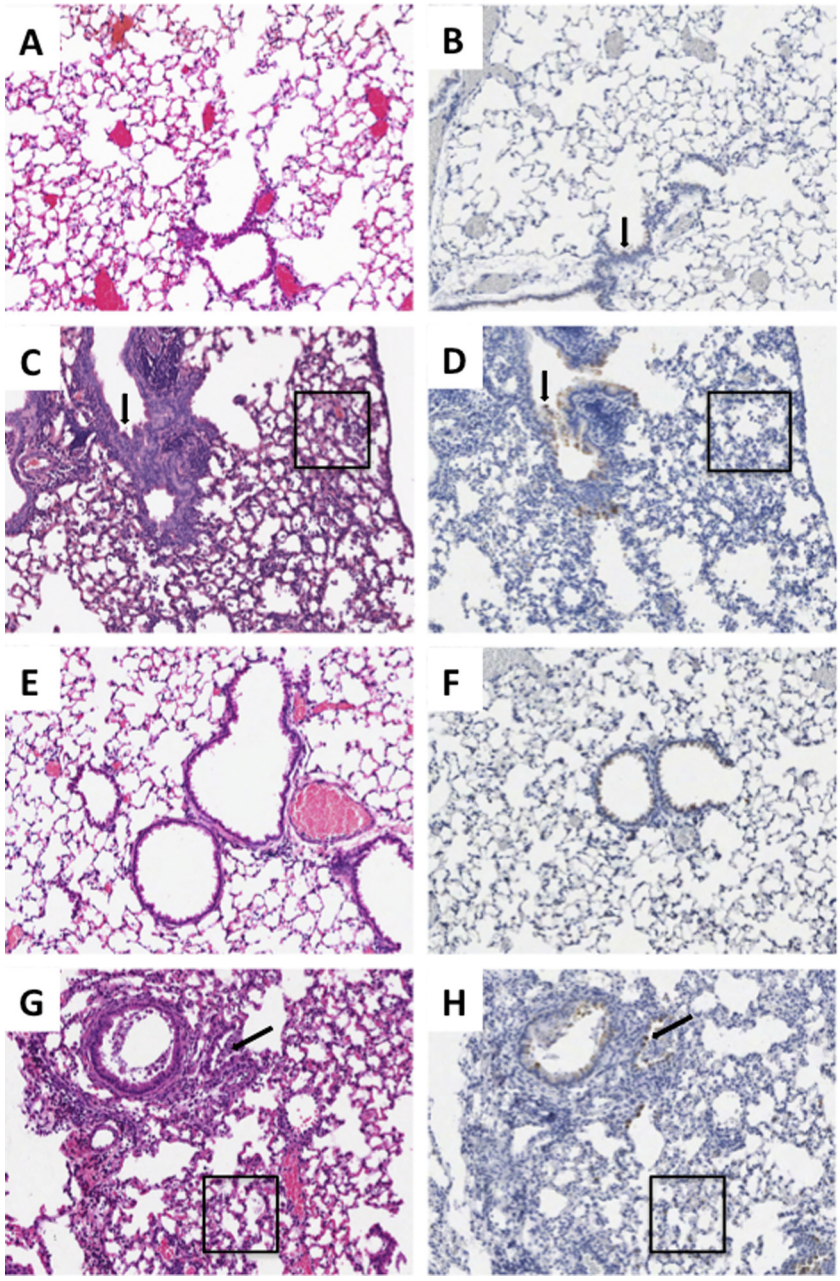

FIG 2 Histopathology and influenza virus antigen distribution for selected viruses. Matched sections of day 5 postinfection lungs (original magnification, ×100). H&E stains are shown in the left column, and influenza virus A antigen immunohistochemistry is shown in the right column with the DAB end product counterstained with hematoxylin. (A and B) Infection with the AI virus, demonstrating the absence of histopathologic changes and influenza virus antigen except rare, multifocal labeling of the bronchial epithelium (arrow). (C and D) Infection with the 1918 virus, showing severe multifocal changes, including transmural necrotizing bronchitis (arrow) and multifocal moderate-to-severe alveolitis with multifocal pulmonary edema (box) and influenza virus antigen in bronchial epithelium (arrow) and alveolar epithelial cells. (E and F) Infection with the $1918^{AI\text{-}PB2}$ virus, showing a similar absence of histopathologic changes comparable to the AI virus, accompanied by slightly stronger labeling of bronchial epithelium. (G and H) Infection with $1918^{AI\text{-}PB2\text{-}K627}$, showing similar histopathology, including transmural necrotizing bronchitis (arrow) and multifocal moderate-to-severe alveolitis with multifocal pulmonary edema (box) and influenza virus antigen distribution in bronchial epithelium and alveolar epithelial cells similar in distribution to the parental 1918 virus.

mammalian adaptation. In this study, however, no attenuation was observed in mice for seven of the eight 1918^{AI} chimeric viruses. The exception was the $1918^{AI\text{-}PB2}$ virus, and this attenuation was corrected by the single PB2 E627K change. This suggests that, in the context of the 7:1 chimeric 1918 viruses, none of the other 56 amino acid changes in the internal proteins in the 1918 virus genome, compared to the AI virus genome (Table 1), were necessary for replication or pathogenicity in BALB/c mice, supporting the functional compatibility of the 1918 genome with gene segments derived from an LPAI virus.

While not the primary goal of the study, the attenuation conferred by the AI PB2 gene reassortant was not unexpected. PB2 has

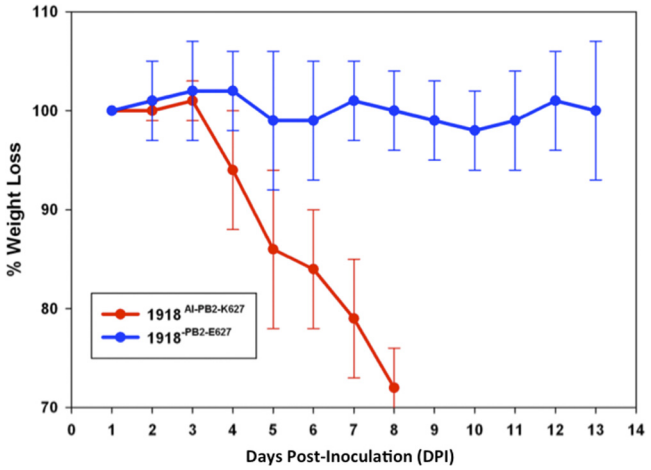

FIG 3 Weight loss of mice infected with PB2-K627E-modified 1918 ($1918^{PB2\text{-}E627}$) and the PB2-E627K-modified 7:1 1918:AI chimeric ($1918^{AI\text{-}PB2\text{-}K627}$) influenza viruses. Seven- to-eight-week female BALB/c mice were intranasally inoculated with 10^3 PFU of the indicated viruses (see Table 2 and color-coded key) and weighed daily (5 mice per virus per group).

long been associated with host restriction (2, 58), and several changes in the C-terminal half of the protein have been associated with mammalian adaptation events, including changes at PB2 codons 627, 701, 702, and more recently 590 and 591 (2, 16, 17, 34, 58, 59, 64, 73). The 1918 virus and its descendant pandemic and seasonal H1N1, H2N2, and H3N2 influenza viruses have maintained the 627K change. This mutation has also been observed and correlated with mouse pathogenicity in some highly pathogenic H5N1 (32, 55) and H7N7 (15) isolates. However, other independently emerged mammalian-adapted influenza viruses lack this change, most notably the pandemic 2009 H1N1 lineage (18, 23, 25, 33), and the Eurasian avian-like swine H1N1 influenza virus lineage (11). Thus, while the 627K change may be critical in the mouse model, it is clearly not the only mechanism for PB2 in mammalian adaptation. The reason that changes in PB2 appear to be a critical requirement for influenza virus mammalian host adaptation remains incompletely understood, but interaction of PB2 with cellular factors has been inferred (6, 14, 35). In published experiments with A/swine/Iowa/1930, an H1N1 virus that is closely related to the 1918 virus, mutation to PB2 627E also attenuated this virus in mice compared to wild-type virus encoding PB2 627K (31). Interestingly, while changes other than PB2 E627K have been observed in naturally evolving mammalian-adapted viruses, and PB2 E627K has been observed in some avian viruses, during the acute mouse infections with the $1918^{AI\text{-}PB2}$ virus, there was rapid selection for the E627K coding change. Sequence analyses of plaque-purified viruses from mouse lung at 5 dpi showed that 92% of the PB2 sequences possessed the E627K change. In a small minority of plaque-purified viruses with the E627K change, another coding change, D611N, was also observed. This change is of unknown significance and may reflect a mouse-adaptive change, as it is not a mutation generally observed in either avian or human influenza viruses. The rapid selection of E627K in this study suggests that either E627K is preferentially associated with mammalian adaptation in the 1918 viral context and/or that this codon is a mutational "hot spot" on the PB2 gene. Interestingly, the AI parental virus did not replicate to detectable titers in mouse lung, suggesting that selection for PB2 E627K in this genomic context did not occur.

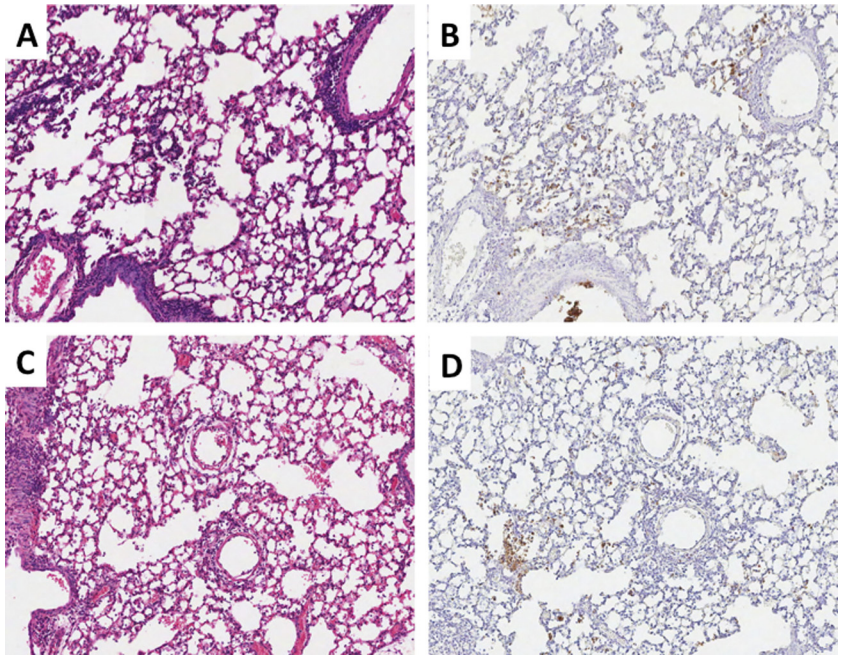

FIG 4 Histopathology and neutrophil distribution for 1918 and $1918^{AI\text{-}HA}$ viruses. Matched sections of day 5 postinfection lungs (original magnification, ×100). H&E stains are shown in the left column, and myeloperoxidase immunohistochemistry is shown in the right column with the DAB end product counterstained with hematoxylin. (A and B) 1918 virus-infected mice, showing severe multifocal changes and numerous myeloperoxidase-positive cells (neutrophils) prominently in the smallest airways, bronchioles, and alveoli. (C and D) $1918^{AI\text{-}HA}$ virus-infected mice, showing similar histopathologic changes to 1918 and a comparable number of neutrophils in correlation with the histopathology.

Neither of the other AI-derived polymerase genes, PB1 and PA, attenuated the 1918 virus in this model. The PB1 gene segments of the 1918, 1957, and 1968 viruses are all very similar to the PB1 gene segments of avian influenza virus, with one possible shared host-adaptive change, N375S (64), but this polymorphism is also seen in wild-type avian influenza viruses. As previously proposed, mammalian-adapted influenza virus polymerase complexes may have higher polymerase activity if they contain an avian influenza virus-derived PB1 gene segment (40). An amino acid change, N66S, in the PB1-F2 protein (encoded by an alternate open reading frame from PB1 on segment 2) has been correlated as a mouse virulence factor in both the 1918 virus and in some H5N1 HPAI virus strains (9). Both the 1918 and AI viruses used in this study encode a serine at position 66 in PB1-F2. The proteins however share only 78.9% identity, consistent with data that PB1-F2 is very divergent in avian influenza viruses and not under strong selection pressure (24). Interestingly, a serine at position 66 is actually the majority amino acid in avian influenza viruses, found in approximately 90% of avian influenza PB1-F2 sequences in GenBank (data not shown). Together, these data suggest that a serine at this site is probably not a mammalian-adaptive mutation but likely reflects the avian consensus sequence at this site. One of the proposed mammalian-adaptive changes in the PA polymerase, T552S, was recently shown to play a role in host switch (36), but since this change is not present in the 2009 pandemic virus, and also because the $1918^{AI\text{-}PA}$ virus encoding T552 was not attenuated in this study, changes in PA from the avian consensus must either be genome context dependent or not critical for mammalian adaptation.

The roles of the remaining influenza virus genes in mammalian host adaptation are less clear (41, 61). Several amino acid changes in NP have been proposed to play a role in host adaptation (13, 41, 51), but since the AI-derived NP did not attenuate the 1918 virus in mice, these changes did not appear critical for replication or pathogenesis in mice, at least in the context of the 1918 genome. In prior studies in which a set of human seasonal influenza A/H3N2 viruses containing single avian influenza virus genes was constructed, the avian influenza virus-derived NP did not attenuate the virus in human volunteer challenge studies but did attenuate replication in squirrel monkeys (8), further supporting the complex and polygenic nature of host adaptation changes. Recent studies have also suggested that specific PB2-NP interactions may be important in host switch events (5), but in the present experiments, the 1918 virus was not attenuated with the AI-derived NP. It remains unclear which mutations might be associated with host adaptation in the NS genes (61). The 1918 NS gene was shown to be a potent inhibitor of antiviral and type I interferon (IFN) responses in cultured human lung cells (19), but it has >98% identity with both NS1 and NEP (NS2) from a number of LPAI sequences. Four changes in the extracellular domain of M2 were proposed to be associated with mammalian adaptation (52), but here again, the AI-derived matrix gene segment lacking these changes did not significantly attenuate the 1918 virus.

While changes in the receptor-binding domain of HA have long been associated with host switch and mammalian adaptation, the significance of these changes for cellular tropism, replication, pathogenicity, and transmissibility remain incompletely understood. Previous studies have shown that viruses expressing different receptor-binding domain configurations in the 1918 HA were similarly pathogenic in mice and ferrets (46, 67). The current study demonstrated that an LPAI-derived H1 without any receptor-binding mutations did not attenuate the 1918 virus in mice, further supporting the hypothesis that α2-6 sialic acid binding specificity is not in itself crucial for mammalian replication in the context of a virus like 1918 that is already mammalian adapted (61).

In addition to its potential importance to host switch, the 1918 HA has been identified as a virulence factor in mice and ferrets (27, 28, 30, 45, 46, 65, 67). Surprisingly, in this study, the AI-derived HA gene did not attenuate the 1918 virus, suggesting that the as yet unknown virulence properties of the 1918 HA might not reflect unique 1918 virus-specific mutations. Instead, this virulence property may be shared with LPAI-derived H1 genes, at least in the context of the 1918 genome in mice. One virulence property that has been associated with all pandemic influenza virus-derived HAs is a low avidity for surfactant protein D, which may correlate with efficient replication in alveolar lining cells (45). While isogenic chimeric seasonal human influenza viruses expressing the HA of the 1918, 1957, 1968, and 2009 pandemics are all more pathogenic in mice than seasonal HA-expressing control viruses (45), only the 1918 HA-expressing viruses induced a neutrophil-predominant alveolitis (45, 46, 65). Whether a similarly constructed seasonal H1N1 influenza virus with the AI-derived H1 HA gene from the current experiment would be pathogenic in mice will be evaluated in future work. Phenotypically, the virulence of viruses expressing the 1918 HA gene has been manifested by a neutrophil-predominant alveolitis (65), whereas other influenza viruses that replicate in the lower respiratory tract tend to induce a more lymphohistiocytic infiltrate (45). Thus, it was also unexpected in this study that the $1918^{AI\text{-}HA}$ virus induced a neutrophil-predominant alveolitis. Future work to understand the biological basis of these observations is planned.

In summary, of the eight 1918-AI chimeras produced, only the $1918^{AI\text{-}PB2}$ virus was attenuated in mice compared to the parental 1918 virus. This attenuation was corrected by the single E627K amino acid change, further confirming the importance of this change in mouse pathogenicity (21, 22). The mechanisms of host switch, and particularly mammalian host adaptation, are still only poorly understood. These data suggest that the genes of the 1918 virus, whatever its origin, are very similar to the genes of avian influenza virus.

ACKNOWLEDGMENTS

This work was supported by the intramural funds of the NIH and the NIAID.

We thank the Comparative Medicine Branch (NIAID, NIH) for assistance with animal studies and the Histopathology Laboratory at the College of Veterinary Medicine of North Carolina State University for assistance with immunohistochemical slide production.

REFERENCES

1. **Alexander DJ, Brown IH.** 2000. Recent zoonoses caused by influenza A viruses. Rev. Sci. Tech. **19**:197–225.
2. **Almond JW.** 1977. A single gene determines the host range of influenza virus. Nature **270**:617–618.
3. **Antonovics J, Hood ME, Baker CH.** 2006. Molecular virology: was the 1918 flu avian in origin? Nature **440**:E9–E10.
4. **Bao Y, et al.** 2008. The influenza virus resource at the National Center for Biotechnology Information. J. Virol. **82**:596–601.
5. **Bogs J, et al.** 2011. Reversion of PB2-627E to -627K during replication of an H5N1 clade 2.2 virus in mammalian hosts depends on the origin of the nucleoprotein. J. Virol. **85**:10691–10698.

6. **Bortz E, et al.** 2011. Host- and strain-specific regulation of influenza virus polymerase activity by interacting cellular proteins. mBio **2**(4):e00151–11. doi:10.1128/mBio.00151–11.
7. **Brownlee GG, Fodor E.** 2001. The predicted antigenicity of the haemagglutinin of the 1918 Spanish influenza pandemic suggests an avian origin. Philos. Trans. R. Soc. Lond. B Biol. Sci. **356**:1871–1876.
8. **Clements ML, et al.** 1992. Use of single-gene reassortant viruses to study the role of avian influenza A virus genes in attenuation of wild-type human influenza A virus for squirrel monkeys and adult human volunteers. J. Clin. Microbiol. **30**:655–662.
9. **Conenello GM, Zamarin D, Perrone LA, Tumpey T, Palese P.** 2007. A single mutation in the PB1-F2 of H5N1 (HK/97) and 1918 influenza A viruses contributes to increased virulence. PLoS Pathog. **3**:1414–1421. doi:10.1371/journal.ppat.0030141.
10. **Dugan VG, et al.** 2008. The evolutionary genetics and emergence of avian influenza viruses in wild birds. PLoS Pathog. **4**:e1000076. doi:10.1371/journal.ppat.1000076.
11. **Dunham EJ, et al.** 2009. Different evolutionary trajectories of European avian-like and classical swine H1N1 influenza A viruses. J. Virol. **83**:5485–5494.
12. **Easterbrook JD, et al.** 2011. Immunization with 1976 swine H1N1- or 2009 pandemic H1N1-inactivated vaccines protects mice from a lethal 1918 influenza infection. Influenza Other Respir. Viruses **5**:198–205.
13. **Finkelstein DB, et al.** 2007. Persistent host markers in pandemic and H5N1 influenza viruses. J. Virol. **81**:10292–10299.
14. **Foeglein A, et al.** 2011. Influence of PB2 host-range determinants on the intranuclear mobility of the influenza A virus polymerase. J. Gen. Virol. **92**:1650–1661.
15. **Fouchier RA, et al.** 2004. Avian influenza A virus (H7N7) associated with human conjunctivitis and a fatal case of acute respiratory distress syndrome. Proc. Natl. Acad. Sci. U. S. A. **101**:1356–1361.
16. **Gabriel G, et al.** 2005. The viral polymerase mediates adaptation of an avian influenza virus to a mammalian host. Proc. Natl. Acad. Sci. U. S. A. **102**:18590–18595.
17. **Gabriel G, Herwig A, Klenk HD.** 2008. Interaction of polymerase subunit PB2 and NP with importin alpha1 is a determinant of host range of influenza A virus. PLoS Pathog. **4**:e11. doi:10.1371/journal.ppat.0040011.
18. **Garten RJ, et al.** 2009. Antigenic and genetic characteristics of swine-origin 2009 A(H1N1) influenza viruses circulating in humans. Science **325**:197–201.
19. **Geiss GK, et al.** 2002. Cellular transcriptional profiling in influenza A virus-infected lung epithelial cells: the role of the nonstructural NS1 protein in the evasion of the host innate defense and its potential contribution to pandemic influenza. Proc. Natl. Acad. Sci. U. S. A. **99**:10736–10741.
20. **Gibbs MJ, Gibbs AJ.** 2006. Molecular virology: was the 1918 pandemic caused by a bird flu? Nature **440**:E8–E10.
21. **Hatta M, Gao P, Halfmann P, Kawaoka Y.** 2001. Molecular basis for high virulence of Hong Kong H5N1 influenza A viruses. Science **293**:1840–1842.
22. **Hatta M, et al.** 2007. Growth of H5N1 influenza A viruses in the upper respiratory tracts of mice. PLoS Pathog. **3**:1374–1379. doi:10.1371/journal.ppat.0030133.
23. **Herfst S, et al.** 2010. Introduction of virulence markers in PB2 of pandemic swine-origin influenza virus does not result in enhanced virulence or transmission. J. Virol. **84**:3752–3758.
24. **Holmes EC, Lipman DJ, Zamarin D, Yewdell JW.** 2006. Comment on "Large-scale sequence analysis of avian influenza isolates." Science **313**:1573. (Reply, 313:1573.)
25. **Jagger BW, et al.** 2010. The PB2-E627K mutation attenuates viruses containing the 2009 H1N1 influenza pandemic polymerase. mBio **1**(1):e00067–10. doi:10.1128/mBio.00067–10.
26. **Johnson NP, Mueller J.** 2002. Updating the accounts: global mortality of the 1918-1920 "Spanish" influenza pandemic. Bull. Hist. Med. **76**:105–115.
27. **Kash JC, et al.** 2004. Global host immune response: pathogenesis and transcriptional profiling of type A influenza viruses expressing the hemagglutinin and neuraminidase genes from the 1918 pandemic virus. J. Virol. **78**:9499–9511.
28. **Kash JC, et al.** 2006. Genomic analysis of increased host immune and cell death responses induced by 1918 influenza virus. Nature **443**:578–581.
29. **Kobasa D, et al.** 2007. Aberrant innate immune response in lethal infection of macaques with the 1918 influenza virus. Nature **445**:319–323.
30. **Kobasa D, et al.** 2004. Enhanced virulence of influenza A viruses with the haemagglutinin of the 1918 pandemic virus. Nature **431**:703–707.
31. **Ma W, et al.** 2011. Pathogenicity of swine influenza viruses possessing an avian or swine-origin PB2 polymerase gene evaluated in mouse and pig models. Virology **410**:1–6.
32. **Mase M, et al.** 2006. Recent H5N1 avian influenza A virus increases rapidly in virulence to mice after a single passage in mice. J. Gen. Virol. **87**:3655–3659.
33. Reference deleted.
34. **Mehle A, Doudna JA.** 2009. Adaptive strategies of the influenza virus polymerase for replication in humans. Proc. Natl. Acad. Sci. U. S. A. **106**:21312–21316.
35. **Mehle A, Doudna JA.** 2008. An inhibitory activity in human cells restricts the function of an avian-like influenza virus polymerase. Cell Host Microbe **4**:111–122.
36. **Mehle A, Dugan VG, Taubenberger JK, Doudna JA.** 2012. Reassortment and mutation of the avian influenza virus polymerase PA subunit overcome species barriers. J. Virol. **86**:1750–1757.
37. **Memoli MJ, et al.** 2009. An early 'classical' swine H1N1 influenza virus shows similar pathogenicity to the 1918 pandemic virus in ferrets and mice. Virology **393**:338–345.
38. **Miotto O, et al.** 2010. Complete-proteome mapping of human influenza A adaptive mutations: implications for human transmissibility of zoonotic strains. PLoS One **5**:e9025. doi:10.1371/journal.pone.0009025.
39. **Morens DM, Taubenberger JK, Fauci AS.** 2009. The persistent legacy of the 1918 influenza virus. N. Engl. J. Med. **361**:225–229.
40. **Naffakh N, Massin P, Escriou N, Crescenzo-Chaigne B, van der Werf S.** 2000. Genetic analysis of the compatibility between polymerase proteins from human and avian strains of influenza A viruses. J. Gen. Virol. **81**:1283–1291.
41. **Naffakh N, Tomoiu A, Rameix-Welti MA, van der Werf S.** 2008. Host restriction of avian influenza viruses at the level of the ribonucleoproteins. Annu. Rev. Microbiol. **62**:403–424.
42. **Pappas C, et al.** 2008. Single gene reassortants identify a critical role for PB1, HA, and NA in the high virulence of the 1918 pandemic influenza virus. Proc. Natl. Acad. Sci. U. S. A. **105**:3064–3069.
43. **Parrish CR, et al.** 2008. Cross-species virus transmission and the emergence of new epidemic diseases. Microbiol. Mol. Biol. Rev. **72**:457–470.
44. **Peiris JSM.** 2009. Avian influenza viruses in humans. Rev. Sci. Tech. **28**:161–173.
45. **Qi L, et al.** 2011. The ability of pandemic influenza virus hemagglutinins to induce lower respiratory pathology is associated with decreased surfactant protein D binding. Virology **412**:426–434.
46. **Qi L, et al.** 2009. Role of sialic acid binding specificity of the 1918 influenza virus hemagglutinin protein in virulence and pathogenesis for mice. J. Virol. **83**:3754–3761.
47. **Rabadan R, Levine AJ, Robins H.** 2006. Comparison of avian and human influenza A viruses reveals a mutational bias on the viral genomes. J. Virol. **80**:11887–11891.
48. **Rambaut A.** 1996. Se-Al: Sequence Alignment Editor. University of Oxford, Oxford, United Kingdom.
49. **Reed LJ, Muench H.** 1938. A simple method of estimating fifty percent endpoints. Am. J. Hyg. **27**:493–497.
50. **Reid AH, Fanning TG, Hultin JV, Taubenberger JK.** 1999. Origin and evolution of the 1918 "Spanish" influenza virus hemagglutinin gene. Proc. Natl. Acad. Sci. U. S. A. **96**:1651–1656.
51. **Reid AH, Fanning TG, Janczewski TA, Lourens RM, Taubenberger JK.** 2004. Novel origin of the 1918 pandemic influenza virus nucleoprotein gene. J. Virol. **78**:12462–12470.
52. **Reid AH, Fanning TG, Janczewski TA, McCall S, Taubenberger JK.** 2002. Characterization of the 1918 "Spanish" influenza virus matrix gene segment. J. Virol. **76**:10717–10723.
53. **Reid AH, Fanning TG, Janczewski TA, Taubenberger JK.** 2000. Characterization of the 1918 "Spanish" influenza virus neuraminidase gene. Proc. Natl. Acad. Sci. U. S. A. **97**:6785–6790.
54. **Reid AH, Taubenberger JK, Fanning TG.** 2004. Evidence of an absence: the genetic origins of the 1918 pandemic influenza virus. Nat. Rev. Microbiol. **2**:909–914.
55. **Shinya K, et al.** 2000. Avian influenza virus intranasally inoculated infects the central nervous system of mice through the general visceral afferent nerve. Arch. Virol. **145**:187–195.
56. **Smith GJ, et al.** 2009. Dating the emergence of pandemic influenza viruses. Proc. Natl. Acad. Sci. U. S. A. **106**:11709–11712.

57. **Smith GJ, et al.** 2009. Origins and evolutionary genomics of the 2009 swine-origin H1N1 influenza A epidemic. Nature **459**:1122–1125.
58. **Subbarao EK, London W, Murphy BR.** 1993. A single amino acid in the PB2 gene of influenza A virus is a determinant of host range. J. Virol. **67**:1761–1764.
59. **Tarendeau F, et al.** 2007. Structure and nuclear import function of the C-terminal domain of influenza virus polymerase PB2 subunit. Nat. Struct. Mol. Biol. **14**:229–233.
60. **Taubenberger JK, Hultin JV, Morens DM.** 2007. Discovery and characterization of the 1918 pandemic influenza virus in historical context. Antivir. Ther. **12**:581–591.
61. **Taubenberger JK, Kash JC.** 2010. Influenza virus evolution, host adaptation, and pandemic formation. Cell Host Microbe **7**:440–451.
62. **Taubenberger JK, Morens DM.** 2006. 1918 influenza: the mother of all pandemics. Emerg. Infect. Dis. **12**:15–22.
63. **Taubenberger JK, Morens DM.** 2009. Pandemic influenza – including a risk assessment of H5N1. Rev. Sci. Tech. **28**:187–202.
64. **Taubenberger JK, et al.** 2005. Characterization of the 1918 influenza virus polymerase genes. Nature **437**:889–893.
65. **Tumpey TM, et al.** 2005. Characterization of the reconstructed 1918 Spanish influenza pandemic virus. Science **310**:77–80.
66. **Tumpey TM, et al.** 2004. Pathogenicity and immunogenicity of influenza viruses with genes from the 1918 pandemic virus. Proc. Natl. Acad. Sci. U. S. A. **101**:3166–3171.
67. **Tumpey TM, et al.** 2007. A two-amino acid change in the hemagglutinin of the 1918 influenza virus abolishes transmission. Science **315**:655–659.
68. **Van Hoeven N, et al.** 2009. Pathogenesis of 1918 pandemic and H5N1 influenza virus infections in a guinea pig model: antiviral potential of exogenous alpha interferon to reduce virus shedding. J. Virol. **83**:2851–2861.
69. **Watanabe T, et al.** 2009. Viral RNA polymerase complex promotes optimal growth of 1918 virus in the lower respiratory tract of ferrets. Proc. Natl. Acad. Sci. U. S. A. **106**:588–592.
70. **Webster RG, Bean WJ, Gorman OT, Chambers TM, Kawaoka Y.** 1992. Evolution and ecology of influenza A viruses. Microbiol. Rev. **56**:152–179.
71. **Weingartl HM, et al.** 2009. Experimental infection of pigs with the human 1918 pandemic influenza virus. J. Virol. **83**:4287–4296.
72. **Wright PF, Neumann G, Kawaoka Y.** 2007. Orthomyxoviruses, p 1691–1740. *In* Knipe DM, Howley PM (ed), Fields virology, 5th ed, vol 2. Lippincott Williams & Wilkins, Philadelphia, PA.
73. **Yamada S, et al.** 2010. Biological and structural characterization of a host-adapting amino acid in influenza virus. PLoS Pathog. **6**:e1001034. doi:10.1371/journal.ppat.1001034.